

Anisotropic universe with anisotropic sources.

Pavan Aluri*, Sukanta Panda†
Manabendra Sharma‡and Snigdha Thakur§

October 12, 2012

Department of Physics, IISER Bhopal, Bhopal-462 023, India

Abstract: We analyze the state space of a Bianchi I universe with anisotropic sources. Here we consider an extended state space which includes null geodesics in this background. The evolution equations for all the state observables are derived. Dynamical system approach is used to study the evolution of these equations. The asymptotic stable fixed points for all the evolution equations are found. We also check our analytic results with numerical analysis of these dynamical equations. The evolution of the state observables are studied both in cosmic time and using a dimensionless time variable. Finally the cosmic microwave background anisotropy maps are generated, assuming that the universe is anisotropic and dominated by one of the anisotropic sources since decoupling. We find that they contribute dominantly to CMB quadrupole.

1 Introduction

In standard cosmology it is assumed that the space-time is homogeneous and isotropic. After the discovery of temperature anisotropies of the Cosmic Microwave Background (CMB) and accelerating expansion of the universe, a standard cosmological model describing universe dominated by cold dark matter (CDM) and cosmological constant (Λ) is formulated, known as Λ CDM model or cosmic concordance model. Fluctuations in the temperature of CMB radiation are statistically isotropic in this model [1, 2]. A central assumption in our standard model of cosmology (and in most cosmological models) is that the universe is homogeneous and isotropic upto small perturbations, and thus described by a perturbed Friedmann-Robertson-Walker (FRW) metric. Observations show that the temperature of the CMB is isotropic to a remarkable degree indicating that our universe is close to an Friedmann-Lemaitre (FL) model. According to Ellis, Geren and Sachs (EGS) theorem [3], if the CMB temperature were exactly isotropic about every point in spacetime, the universe would have to be exactly an FL model. This result is not directly applicable to CMB, because, CMB radiation is not exactly isotropic. The presence of this feature in the observations of temperature anisotropies of the CMB those from Wilkinson Microwave Anisotropy Probe (WMAP) seems to be inconsistent with a homogeneous and isotropic FRW model. It may be evidence that we live in a globally anisotropic universe.

*email: pavan@iiserb.ac.in

†email: sukanta@iiserb.ac.in

‡email: manabendra@iiserb.ac.in

§email: snigdha@iiserb.ac.in

The current CMB data supports an inflationary Big Bang model of cosmic origin for our universe. However at large angular scales, there are some anomalies observed in CMB data, such as, a low value for quadrupole power, alignment of quadrupole and octopole modes roughly in the direction of virgo cluster, ecliptic north-south power asymmetry, parity asymmetry between even and odd multipoles, almost zero correlations on large angular scales of CMB and an anomalous cold spot (10° diameter) in the southern galactic hemisphere of CMB sky [4]. Several other solutions to low multipole CMB anomalies can be found, for example in Ref. [5]. Some these supposed deviations seen in CMB data were addressed by the WMAP science team in Ref. [6].

Generally, in a global anisotropic universe, during inflation shear decreases and eventually it goes over to an isotropic phase with negligible shear. In order to produce any substantial amount of shear in recent times one needs to induce anisotropy in the spacetime. One way to induce anisotropy is to have anisotropic matter present at the last scattering surface. It was shown earlier that power suppression in CMB quadrupole without affecting higher multipoles, can be explained by assuming anisotropic matter [7, 8]. The sources for these matters can be uniform magnetic field, cosmic strings or a domain walls. A nanogauss scale magnetic field could be present today which would have been produced during inflation due to a lorentz-violating term to the photon sector [9]. We call matter in this form as “Lorentz-Violating magnetic field(LVMF)”.

In this paper our approach is not to deal with metric approach directly, but rather to adhere to an approach similar to orthonormal frame formalism [10]. This paper is organised as follows. In section 2, we write down the Einstein’s equations in cosmic time. Geodesic equations in cosmic time are studied in section 3. In section 4, we do a fixed point analysis of all the evolution equations in terms of a dimensionless time variable (τ), to study the asymptotic evolution of the state observables. Finally, in section 6, we show the temperature patterns for CMB due to various anisotropic sources considered in our study.

2 Bianchi I universe

The way we study dynamical systems is that we first write evolution equations in terms of few dimensionless state observables. It is a very invaluable tool to obtain qualitative information about the solution about the state space of Bianchi universes((see ref. [10] and references therein). Here we concentrate only on Bianchi 1 model. First we derive the Einstein equations in metric approach. Then we write in terms of state observable analogous to orthonormal frame formalism([11]. In this approach one writes the field equations as first order differential equations. An advantage of this approach is that the derivation of geodesic equation is easy compared to the metric approach.

We start with a Bianchi I line element with a residual planar symmetry in the $y - z$ plane as

$$ds^2 = dt^2 - a(t)^2 dx^2 - b(t)^2 (dy^2 + dz^2). \quad (1)$$

We choose the diagonal energy momentum tensor of the form $T_\nu^\mu = (\rho, -p_a, -p_b, -p_b)$, where $p_a = w_a \rho$ and $p_b = w_b \rho$. The four kinds of anisotropic matter we study here are given in Table 1.

Einstein equations for the metric given in Eq.[1] are

$$2H_a H_b + H_b^2 = 8\pi G \rho, \quad (2)$$

Matter	w_a	w_b
Magnetic Field	-1	1
Cosmic String	-1	0
Domain Walls	0	-1
LVMF	1	0

Table 1: Matter content for different anisotropic sources considered in this paper.

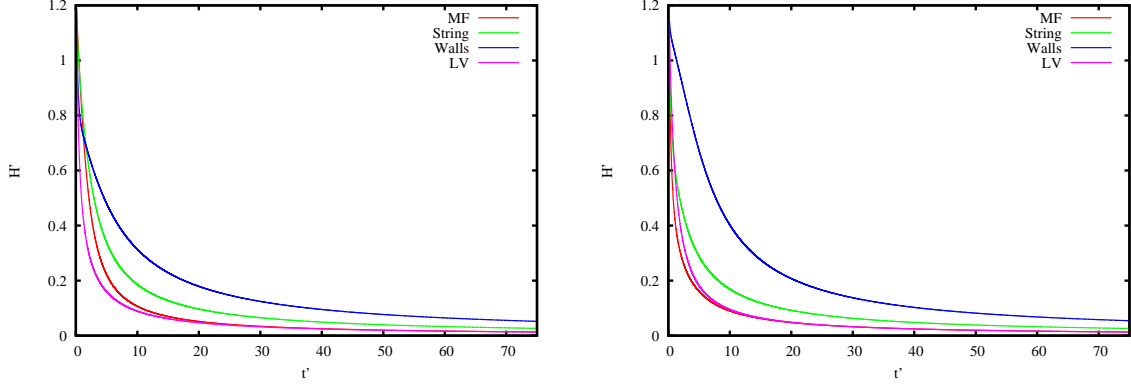


Figure 1: H' vs. t' . In the *left* figure, $h'(0) = 173, h_0/H_0 = 0.01, \Omega_0 = 0.1, \rho'(0) = 10$, and in the *right* figure $h'(0) = -173, h_0/H_0 = 0.01, \Omega_0 = 0.1, \rho'(0) = 10$.

$$2\dot{H}_b + 3H_b^2 = -8\pi G p_a, \quad (3)$$

$$\dot{H}_a + \dot{H}_b + H_a^2 + H_a H_b + H_b^2 = -8\pi G p_b, \quad (4)$$

with $H_a = \frac{1}{a} \frac{da}{dt}$ and $H_b = \frac{1}{b} \frac{db}{dt}$. The equation of continuity is given by,

$$\dot{\rho} + (H_a + 2H_b)\rho + H_a p_a + 2H_b p_b = 0. \quad (5)$$

Here now onwards we choose to set $8\pi G = 1$ for the rest of this paper. This can be otherwise be seen as rescaling, all the quantities in Eq.[2, 3, 4] with $1/\sqrt{8\pi G}$. Now, we rewrite the above set of equations Eq.[2, 3, 4], [5] in terms of the average expansion $H = \frac{H_a + 2H_b}{3}$ and shear $h = \frac{H_a - H_b}{\sqrt{3}}$. The Einstein's equations and the equation of continuity in cosmic time becomes

$$\frac{dH}{dt} = -H^2 - \frac{2}{3}h^2 - \frac{1}{6}(\rho + p_a + 2p_b), \quad (6)$$

$$\frac{dh}{dt} = 3hH + \frac{1}{\sqrt{3}}(p_b - p_a), \quad (7)$$

$$\frac{d\rho}{dt} = -3H\left(\rho + \frac{p_a + 2p_b}{3}\right) + 2\frac{h}{\sqrt{3}}(p_b - p_a) \quad (8)$$

and the constraint equation can be expressed as

$$H^2 = \frac{\rho}{3} + \frac{h^2}{3}. \quad (9)$$

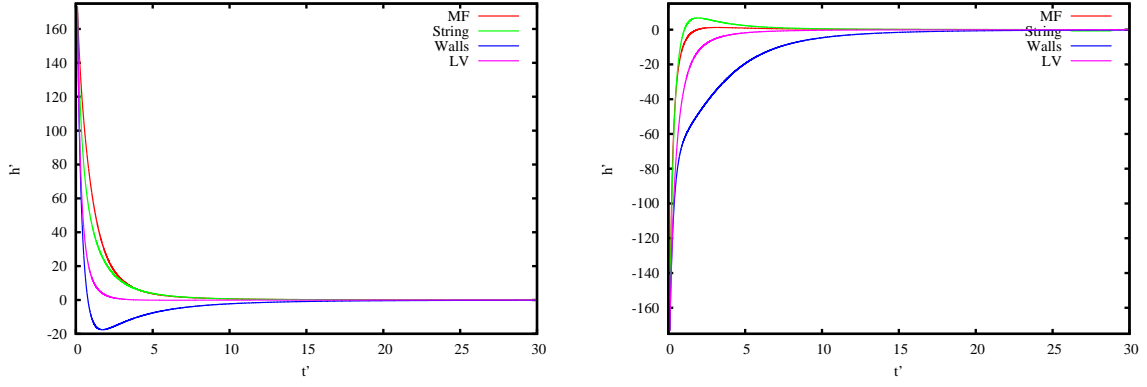


Figure 2: h' vs. t' . In the *left* figure, $h'(0) = 173, h_0/H_0 = 0.01, \Omega_0 = 0.1, \rho'(0) = 10$, and in the *right* figure $h'(0) = -173, h_0/H_0 = 0.01, \Omega_0 = 0.1, \rho'(0) = 10$.

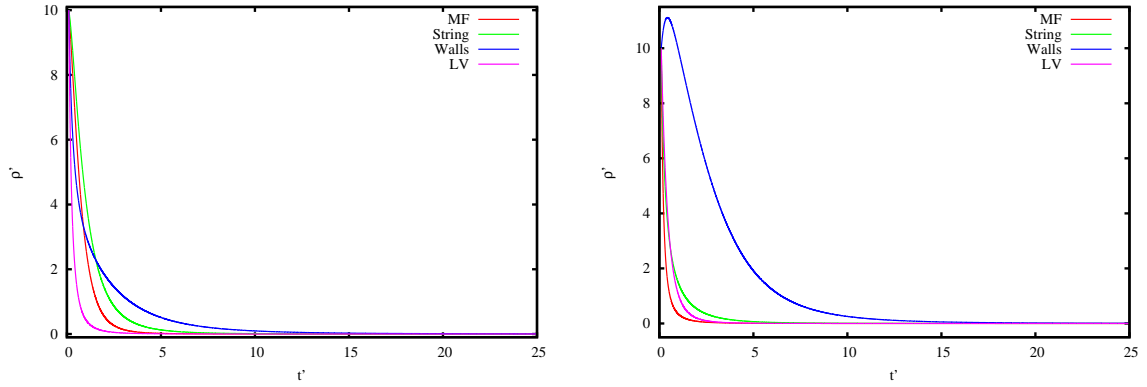


Figure 3: ρ' vs. t' . In *left(right)* figure, the initial data is same as in *left(right)* figures of Fig. [1], respectively.

We now introduce dimensionless variables H' , h' , t' defined as

$$H' = \frac{H}{H_0}, \quad (10)$$

$$h' = \frac{h}{h_0}, \quad (11)$$

$$t' = tH_0, \quad (12)$$

$$\rho' = \frac{\rho}{\rho_0} \quad (13)$$

where H_0 and h_0 are the current value of hubble and shear parameter respectively. Then the equations for the state observables in terms of these dimensionless variables can be written as

$$\dot{H}' = -H'^2 - \frac{2}{3}(h_0/H_0)^2 h'^2 - \frac{1}{2}(1 + w_a + 2w_b)\Omega_0\rho', \quad (14)$$

$$\dot{h}' = 3h'H' + \frac{1}{\sqrt{3}}(w_b - w_a)\Omega_0\rho', \quad (15)$$

$$\dot{\rho}' = -3H'(1 + \frac{w_a + 2w_b}{3})\rho' + 2\frac{h_0}{H_0}\frac{h'}{\sqrt{3}}(w_b - w_a)\rho', \quad (16)$$

where overdot represents differentiation with respect to t' and $\Omega_0 = \frac{\rho_0}{3H_0^2}$. Now, we solve the above equation numerically for all the cases listed in Table. 1. The evolution of the dynamic variables H' , h' and ρ' are plotted in Fig. [1], [2] and [3]. For all these anisotropic matter sources, it turns out that H' decreases with increasing time t' . Uniform magnetic field and LVMF matter have almost similar rate of expansion, where as walls and strings have a higher rate of expansion. Similarly from Fig. [2] we see that isotropy can be attained at late times for all cases of anisotropic matter and shear becomes negligible at late times. Here we find that isotropy sets in much later for walls compared to the other three sources. Except for walls, in all other cases isotropy is achieved almost at the sametime. We observe from Fig. [3] that, the energy density also decreases much faster for magnetic field, LVMF and strings compared to walls. From Fig. [2], it can be observed that evolution of shear depends on the initial conditions. Signature change of shear can be seen for certain kind of anisotropic matter. This signature change may have implications in early universe. From the left plot of Fig. [2], we see that this change occurs for walls, whereas right plot of Fig. [2] shows a similar signature change but for cosmic strings, depending on a positive/negative shear in the beginning. However late time behaviours of H' , h' , ρ' in cosmic time are independent of initial conditions.

3 Null Geodesics in cosmic time t'

As we know the geodesic equations are of second order differential equations in metric approach. If we represent the same equation in terms of H and h , then the geodesics can be written as first order differential equations which are given by [12]

$$\dot{\epsilon} = -H\epsilon - \frac{(\epsilon^2 - 3k_1^2)h}{\sqrt{3}\epsilon}, \quad (17)$$

$$\dot{k}_1 = \left(-H + 2\frac{h}{\sqrt{3}}\right)k_1, \quad (18)$$

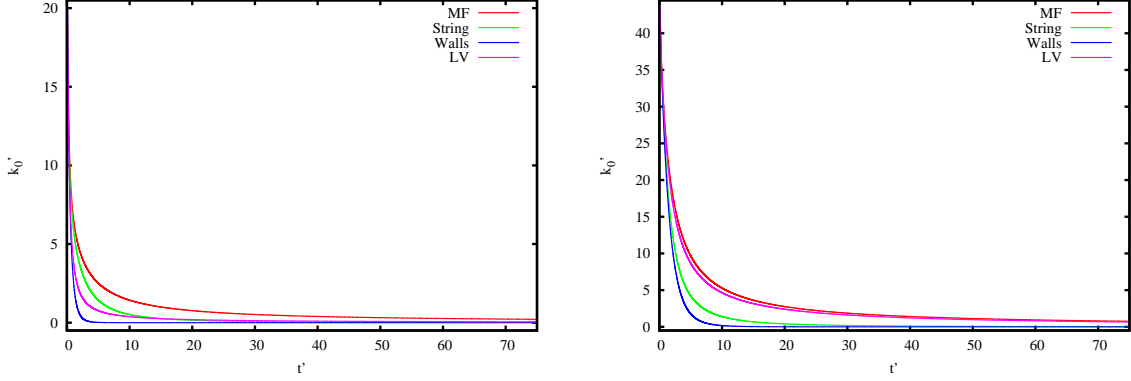


Figure 4: k_0 vs. t' The initial data is same as in Fig. [1] and (left) $\epsilon(0) = k_0 = 20$ (Case 1) and (right) $k_1(0) = k_3(0) = 25.3$ (Case 2).

$$\dot{k}_2 = \left(-H - \frac{h}{\sqrt{3}}\right) k_2, \quad (19)$$

$$\dot{k}_3 = \left(-H - \frac{h}{\sqrt{3}}\right) k_3, \quad (20)$$

where $\epsilon = k_0$ is the energy of photon, k_1 , k_2 and k_3 are the three components of photon momentum. The variables ϵ and k_i ($i=1,2,3$) satisfies the constraint equation

$$\epsilon^2 = k_i k^i. \quad (21)$$

In terms of cosmic time t' the above equations become

$$\dot{\epsilon} = -H'\epsilon - \frac{h_0}{H_0} \frac{(\epsilon^2 - 3k_1^2)h'}{\sqrt{3}}, \quad (22)$$

$$\dot{k}_1 = \left(-H' + 2\frac{h_0}{H_0} \frac{h'}{\sqrt{3}}\right) k_1, \quad (23)$$

$$\dot{k}_2 = \left(-H' - \frac{h_0}{H_0} \frac{h'}{\sqrt{3}}\right) k_2, \quad (24)$$

$$\dot{k}_3 = \left(-H' - \frac{h_0}{H_0} \frac{h'}{\sqrt{3}}\right) k_3, \quad (25)$$

In order to solve the null geodesics Eq. [25], one needs to take care that the solutions should satisfy the constraint equation Eq. [21]. We solve the geodesic equations numerically for two particular cases.

Case 1 : In this case only k_1 is taken to be nonzero and k_2 and k_3 are zero. Initial values of $k_1(0) = 20eV$ and $k_2(0) = k_3(0) = 0$ are taken. The constraint equation Eq. [21] gives $k_1 = \pm k_0 = \pm \epsilon$. Here we choose the positive value for k_0 . The plot for k_0 are shown in left of Fig. 4 for only initial values of $k_0(0) = 20$. Here we find that if initial value of k_0 is positive then for entire evolution it remains positive. It's also true for negative initial values of k_0 . Other initial values are same as Fig. [1], [2] and [3]. We observe that k_0 decreases slowly for magnetic field and faster for walls. This can be observed from Fig. [1] where H' decreases slowly for walls and faster for a magnetic field. Higher expansion rate means lower energy. Hence the above

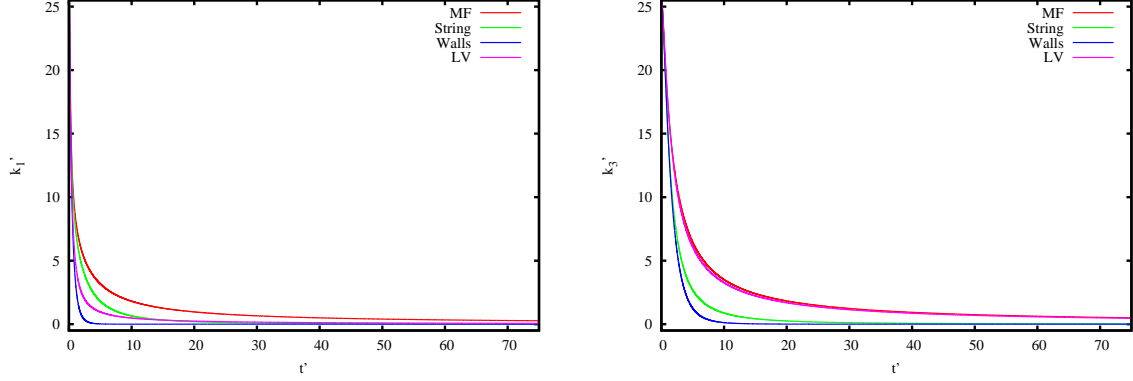


Figure 5: Shown here are *left* k_1 vs. t' and *right* k_3 vs. t' . The initial data is same as in Fig. [1] and $k_1(0) = k_3(0) = 25.3$. These are plotted for Case 2.

analysis is consistent.

Case 2: In this case $k_1(0) = k_3(0) = 25.3$. Other initial values are same as Case 1. The plots for k_1 and k_3 are shown in Fig. [5]. In this case we also observe that k_0 decreases slowly for magnetic field and faster for walls, where as k_1 decreases faster in case of walls and slowly in case of walls.

4 Fixed point analysis of the evolution equations

In the previous section we studied the evolution of state observables in terms of a time variable analogous to cosmic time. In order to study the asymptotic evolution of our Bianchi I universe with various anisotropic sources considered here, we resort to dynamic systems approach. So, we cast all the evolution equations in terms of dimensionless variables which give us a set of dynamical equations. The advantage of working in this approach is that we can show the cosmological dynamics insensitive to the initial conditions. Here we define the dimensionless variables τ, σ as $d\tau/dt = H$ and $\sigma = h/\sqrt{3}H$. These can be called as expansion normalised time and shear variables. Thus our Einstein's equations and the continuity equation are given by

$$\frac{dH}{d\tau} = -H(1+q), \quad (26)$$

$$\frac{d\sigma}{d\tau} = -3(1-\sigma^2) \left[\frac{1}{2}(1-w)\sigma - (w_b - w) \right] \quad (27)$$

and

$$\Omega + \sigma^2 = 1 \quad (28)$$

where $q = 2\sigma^2 + (1+3w)/2\Omega$, $w = (w_a + 2w_b)/3$ and $\Omega = \rho/3H^2$.

Next, we write the (null) geodesic equations in terms of dimensionless variables $K_i = k_i/k_0 (i = 1, 2, 3)$. They are given by

$$\frac{d\epsilon}{d\tau} = (1+s)\epsilon, \quad (29)$$

Matter	σ	(K_1, K_2, K_3)
Magnetic Field	1	$(\pm 1, 0, 0)$
Cosmic String	1/2	$(\pm 1, 0, 0)$
Domain Walls	-2/5	$(0, \pm 1/\sqrt{2}, \pm 1/\sqrt{2})$
LVMF	-1	$(0, \pm 1/\sqrt{2}, \pm 1/\sqrt{2})$

Table 2: Stable fixed points of the whole state space.

$$\dot{K}_1 = (s + 2\sigma)K_1, \quad (30)$$

$$\dot{K}_2 = (s - \sigma)K_2, \quad (31)$$

$$\dot{K}_3 = (s - \sigma)K_3, \quad (32)$$

where $s = (1 - 3K_1^2)\sigma$. The variables K_i ($i=1,2,3$) satisfy the constraint equation

$$K_i K^i = 1. \quad (33)$$

Here we will analyze the fixed points of the full set of equations combining Einstein equations, equation of continuity and the geodesic equations [12]. Fixed points for σ can be easily obtained from Eq. [27] which are +1,-1 and $2(w_b - w)/(1 - w)$. All the stable fixed points are given in Table [2]. Same conclusion can be drawn from solving these equations numerically. The evolution of σ and K_1 and K_3 are plotted in Fig. [6] and [7]. For *positive* τ , we can see that σ evolves towards its stable fixed points while K_1 and K_3 evolves towards their corresponding stable fixed points. This whole analysis is independent of the initial conditions. Exact solutions corresponding to fixed points of σ can be derived with the method as described in appendix of ref. [13].

5 Temperature Patterns

Assuming that the universe is a Bianchi type I and dominated by an anisotropic matter, we find the contribution to the CMB anisotropies due to these sources. It has been shown earlier that the total quadrupole anisotropy in the presence of a uniform magnetic field, can be made small compared to that obtained with isotropic sources in standard Λ CDM model [7]. The temperature of the cosmic microwave background as function of angular coordinates (θ, ϕ) on the celestial sphere is given by [14],

$$T(\theta, \phi) = T_{LSS} \frac{e^{\tau_0 - \tau_{LSS}} e^{2A_0}}{\sqrt{e^{6A_0} + (1 - e^{6A_0}) \cos^2 \theta}}, \quad (34)$$

where T_{LSS} is the temperature of the cosmic microwave background at the surface of last scattering. τ_0 and τ_{LSS} are the values of τ at today and at the time of last scattering surface and

$$A_0 = \int_{\tau_{LSS}}^{\tau_0} \sigma d\tau. \quad (35)$$

Here we have taken $\tau_0 = 0$ and $\tau_{LSS} = -7$. It turns out that the quadrupole contribution is dominant for all the four cases of anisotropic matter considered here. The CMB quadrupole

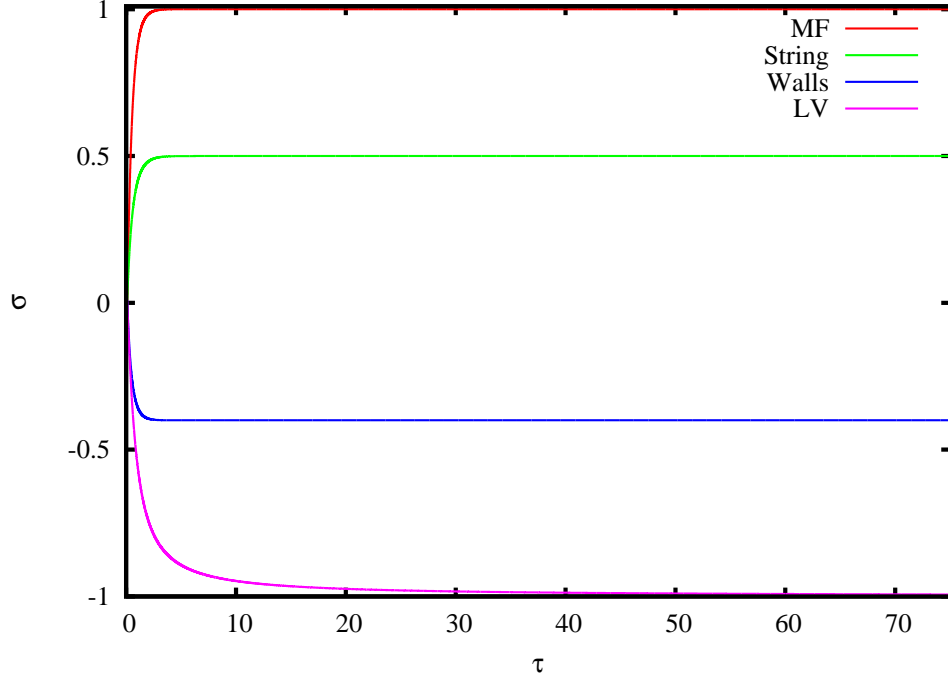


Figure 6: σ vs τ .

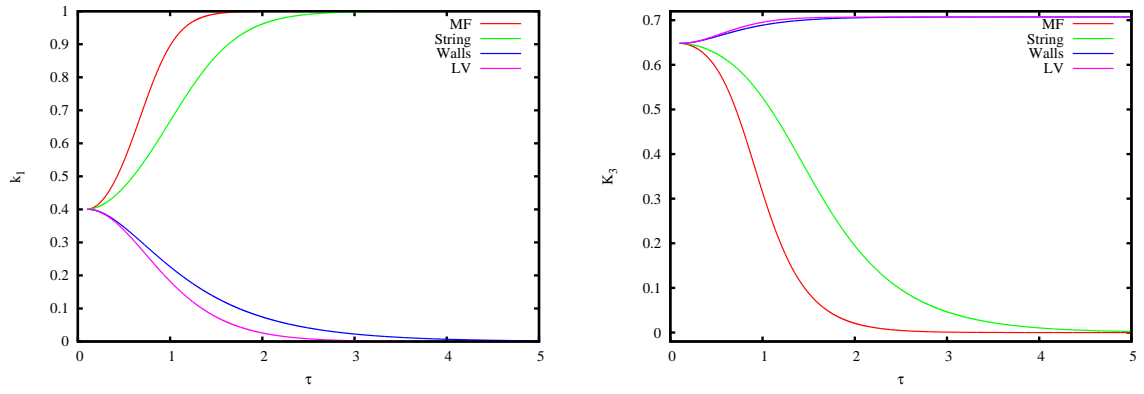


Figure 7: *Left* K_1 vs. τ , and *Right* K_3 vs. τ . Here initial value $\sigma = .01$ is taken.

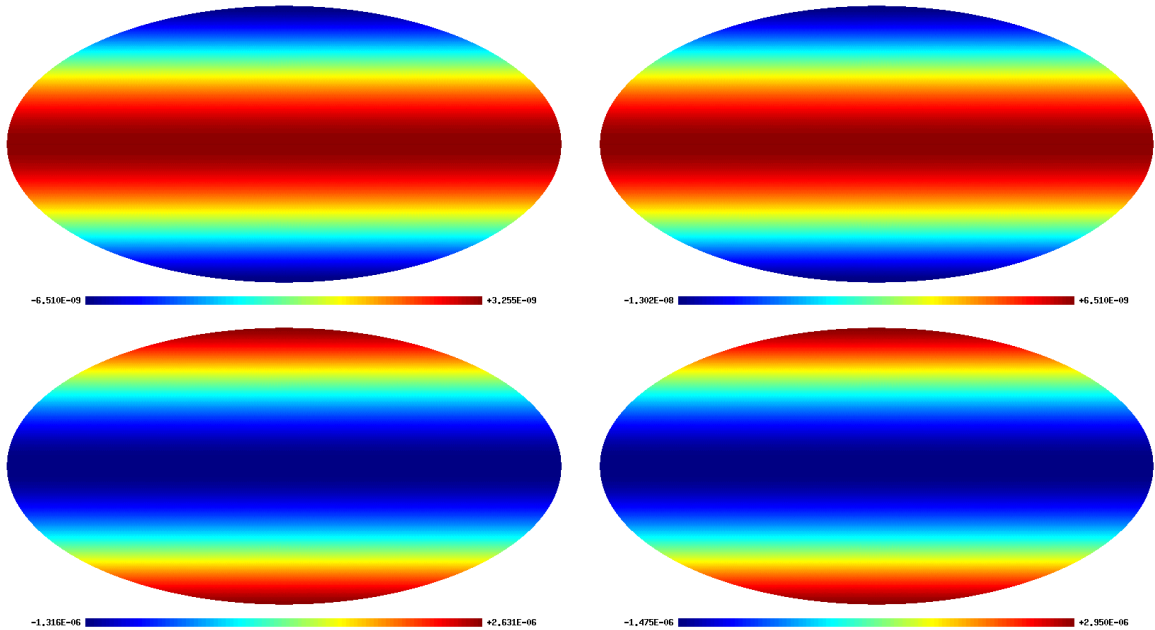


Figure 8: Temperature patterns $\frac{T(\theta, \phi)}{T_{LSS}}$ for Magnetic field (*top left*), Cosmic Strings (*top right*), Domain walls (*bottom left*), and LVMF (*bottom right*). Here we have taken $\sigma(0) = 10^{-5}$.

temperature patterns are given in Fig. [8]. We find that all other higher multipoles receive negligible contribution due to these sources. That is why here we only show temperature patterns for $l = 2$ only. We also observe from Fig. [8] that temperature maps for magnetic field and cosmic strings are of similar patterns and whereas temperature maps for domain walls and LVMF show similar patterns. This can be understood from the evolution of σ given in Fig. [6]. The value of σ stays positive for the entire evolution in case of magnetic field and cosmic string where as it becomes negative for the entire evolution in case of walls and LVMF.

6 Conclusions

Here we study the evolution of Bianchi-I universe in the presence of different types of anisotropic matters. First we see the evolution of the state space variables $H', h', \rho', k_0, k_1, k_3$ in cosmic time. Depending on the initial conditions we can have sign change in observable like shear. This may have some applications in early cosmology. Then we examine the evolution in terms of dimensionless variables like σ, K_1, K_3 in dimensionless time τ . In the τ - frame we find the fixed points of the full set of evolution equations including geodesic equations. We also check the stability of the fixed points numerically. In τ time the temperature of the CMB can be written in a very simple manner. Finally we generate the temperature patterns of the CMB for four different types of anisotropic matter considered here. We find that the contribution to CMB temperature patterns mainly coming from quadrupole. We also pointed out the difference between the CMB temperature maps due to all the cases of anisotropic matter.

Here we have not constrained parameters like shear in these models from CMB data. It will be interesting to generalise our result to other Bianchi class A and B models. In case of other

Bianchi models the state space would be larger and we need to find different subspace of state space and their stable fixed points. It will also be interesting to study the CMB polarisation anisotropy in these models.

Acknowledgements : S.T would like to acknowledge Department of Science and Technology, India for financial support.

References

- [1] C. L. Bennett *et al.* [WMAP Collaboration], *Astrophys. J. Suppl.* **148**, 1 (2003) [astro-ph/0302207].
- [2] G. Hinshaw *et al.* [WMAP Collaboration], *Astrophys. J. Suppl.* **180**, 225 (2009) [arXiv:0803.0732 [astro-ph]].
- [3] J. Ehlers, P. Geren, R. .K. Sachs, O. Verkhodanov, *J.Math.Phys* **9**, 1344 (1968).
- [4] G. Hinshaw *et al.*, *Astrophys. J. Suppl.* **148**, 135 (2003). G. Efstathiou, *MNRAS.* **346**, L26 (2003). M. Tegmark, A. de Oliveira-Costa and A. J. Hamilton, *Phys. Rev. D.* **68**, 123523 (2003). A. de Oliveira-Costa *et. al.*, *Phys. Rev. D* **69**, 063516 (2004). J. P. Ralston and P. Jain, *Int. J. Mod. Phys. D* **13**, 1857 (2004). D. J. Schwarz *et al.*, *Phys. Rev. Lett.* **93**, 221301 (2004). H. K. Eriksen *et. al.*, *Astro. Phys. J.* **605**, 14 (2004). F. K. Hansen *et. al.*, *Astro. Phys. J.* **704**, 1448 (2004). D. Hanson and A. Lewis, *Phys. Rev. D.* **80**, 063004 (2009). K. Land and J. Magueijo, *Phys. Rev. D.* **72**, 101302 (2009). J. Kim and P. Naselsky, *Phys. Rev. D.* **82**, 063002 (2010). P. K. Aluri and P. Jain, *MNRAS.* **419**, 3378 (2012) D. N. Spergel *et al.*, *Astrophys. J. Suppl.* **148**, 175 (2003) C. Copi *et al.*, *Phys. Rev. D.* **75**, 023507 (2007). P. Vielva *et. al.*, *Astro. Phys. J.* **609**, 22 (2004)
- [5] A. Slosar and U. Seljak, *Phys. Rev. D.* **70**, 083002 (2004). E. F. Bunn and A. Bourdon, *Phys. Rev. D.* **78**, 123509 (2008). P. K. Aluri *et. al.*, *MNRAS.* **14**, 1032 (2010). A. Berera, R. V. Buniy and T. W. Kephart, *JCAP.* **10**, 16 (2004). J. W. Moffat, 2005, *JCAP.* **10**, 12 (2005). C. Gordon *et al.*, *Phys. Rev. D.* **72**, 103002 (2005). L. Ackerman, S. M. Carroll and M. B. Wise, *Phys. Rev. D.* **75**, 083502 (2007). R. Sung, J. Short and P. Coles, *MNRAS.* **412**, 492 (2011). P. K. Aluri and P. Jain, *Mod. Phys. Lett. A.* **27**, 1250014 (2012). G. Efstathiou, Y-Z. Ma and D. Hanson, *MNRAS.* **407**, 2530 (2010). R. Aurich and S. Lustig, *MNRAS.* **411**, 124 (2011). C. J. Copi *et al.*, *MNRAS.* **418**, 505 (2011). S. M. Feeney, H. V. Peiris and A. Pontzen, *Phys. Rev. D.* **84**, 103002 (2011).
- [6] C. Bennett *et.al.*, *ApJS*, 192, 17 (2011)
- [7] L. Campanelli, P. Cea and L. Tedesco, *Phys. Rev. Lett.* **97**, 131302 (2006) [Erratum-*ibid.* **97**, 209903 (2006)] [astro-ph/0606266].
- [8] L. Campanelli, P. Cea and L. Tedesco, *Phys. Rev. D* **76**, 063007 (2007) [arXiv:0706.3802 [astro-ph]].
- [9] L. Campanelli, *Phys. Rev. D* **80**, 063006 (2009) [arXiv:0907.3703 [astro-ph.CO]].
- [10] Wainwright, J. and Ellis, G. F. R. (1997). *Dynamical systems in cosmology* (Cambridge University Press, Cambridge).

- [11] Ellis, G. F. R. and MacCallum, M. A. H. (1969). *Commun. Math. Phys.* **12**, 108.
- [12] U. S. Nilsson, C. Uggla and J. Wainwright, *Gen. Rel. Grav.* **32**, 1319 (2000) [gr-qc/9908062].
- [13] S. Calogero and J. M. Heinzle, *Physica D* **240**, 636 (2011) [arXiv:0911.0667 [gr-qc]].
- [14] W. C. Lim, U. S. Nilsson and J. Wainwright, *Class. Quant. Grav.* **18**, 5583 (2001) [gr-qc/9912001].